

Scale-up and Design of the Janicki Omniprocessor with Reverse Osmosis Technology

A Technical Report for CHE 4476

Presented to the Faculty of the School of Engineering and Applied Sciences
University of Virginia • Charlottesville, Virginia

In Partial Fulfillment of the Requirements for the Degree
Bachelor of Science in Chemical Engineering

Author

Adam Mann
May 11, 2021

Technical Project Team Members

Julia George
Noah Sprouse
Arthur Wu

On my honor as a University Student, I have neither given nor received unauthorized aid
on this assignment as defined by the Honor Guidelines for Thesis-Related Assignments

Signature: Adam Mann Date May 11, 2021

Approved _____ Date _____

Eric Anderson, Department of Chemical Engineering

Table of Contents

1. Summary	2
2. Introduction	4
3. Previous Work	6
4. Discussion	7
4.1. Project Scale	7
4.2. Reactor Equipment	7
4.3. Modeling the Combustion Reactor in Aspen	8
4.4. Modeling Feedstock Components	9
4.5. Furnace Simulation Results	12
4.6. Steam Loop Simulation	13
4.7. Separations and Water Purification Simulation	17
4.8. Drying Ponds	32
5. Final Recommended Design	33
6. Health and Environmental Safety	43
7. Conclusion	46
8. Acknowledgements	49
9. Appendix	50
Appendix A. Calculations	50
Appendix B. Equations	52
Appendix C. Tables of Data	53
10. References	57

1. Summary

The scale up of the Janicki Omniprocessor (JOP) requires several unit operations and intermediate steps that will ultimately produce potable water, electric power, and fertilizing ash. Currently, a JOP pilot plant exists in Dakar, Senegal with the capacity to process the waste of 100,000 humans. However, since 1,000,000 residents of Dakar lack adequate sanitation services, we scaled our project to provide for a population of that size.

The Janicki Omni Processor is an innovative waste treatment plant that combines three well-proven processes into one project. Beginning with solid fuel combustion, wet biosolids obtained from mainly pit latrines enter a dryer where the moisture is evaporated in drying ponds prior to entering the furnace. The dried solid waste becomes fuel that is burned in the furnace, producing dry fly ash, or fertilizing ash, becoming the first product. The exhaust gas from the combustion contains materials that may be potentially harmful for the environment, but can be filtered to meet regulations before being released to the environment, and is seen as out-of-scope for this system. The heat that is generated in the furnace is utilized to generate high-pressure, high-temperature steam which is then sent to a steam turbine to produce electricity, the second product. This electricity is used to power the JOP and if extra is produced, it can be supplied to the utility grid locally for other processes. The steam, now at a lower pressure, travels back to the heat exchanger within the dryer where it provides the energy to dry the incoming wet biosolids. As the heat is transferred back, the steam is condensed back to water and pumped back to the heat exchanger in the furnace, completing the steam cycle. The water that is then evaporated from the wet waste is obtained and filtered before being condensed back to water, the third and final product.

The human feces will not cost anything as the process will become a service for the city, while the three products will have prices which will accumulate to over 4,000,000 USD annually as revenue. We achieved a current internal rate of return of 14.5% through a discounted cash flow analysis assuming a 20-year plant life-span. Thus, the execution and investment of this JOP process are deemed profitable for future ventures.

2. Introduction

According to the World Health Organization, the improper treatment and disposal of human waste from 4.5 billion people worldwide has led to the recent rise of polio, cholera, and numerous other diarrheal diseases (Burga, n.d.). Many of these diseases are most widespread in countries where toilets are emptied into local rivers without any clear system for managing the waste. Around 700,000 children die every year due to the diseases caused by poor sanitation (Chowdhry, 2015). Additionally, 783 million people are living without clean water and approximately 2.5 billion do not have access to acceptable sanitation. The United Nations (U.N.) predicts that by 2030, almost half of the planet's population will face water scarcity, a reality of which many are unaware (Poon, 2015). The JOP technology could improve the living conditions of millions of people by providing the basic human right to clean water while also offering sustainable energy.

The JOP was invented by Peter Janicki and developed by Sedron Technologies with funding from the Gates Foundation. The primary goal of the JOP is to render fecal sludge pathogen-free in order to stop the spread of disease in an economically sustainable way. Adequate sanitation is fundamentally crucial to human health, yet the infrastructure required for industry-standard solutions proves cost prohibitive for much of the world's population. This process rethinks waste management facilities to increase efficiency and lower operation cost with the intention of deploying this process to areas of the world where sufficient wastewater management remains nonexistent (Burga, n.d.). The innovative aspect of the JOP is its ability to simultaneously provide three valuable products on top of wastewater treatment: drinking water, electricity, and fertilizing ash. Advancements like this are necessary for areas that need clean

water and proper sanitation. Other plants usually burn waste by using diesel, and therefore consume copious amounts of energy. By contrast, the JOP uses a steam engine which claims to produce more than enough energy to power itself and provide spare electricity (Chowdhry, 2015). The JOP technology has the ability to treat increasing amounts of city sewage through scale-up and process optimization.

While the JOP was first built in Washington state, the real operation of the JOP project took place in Dakar, Senegal, which came with a different set of complications (*Project Overview / Sedron Technologies*, n.d.). In May of 2015, when the pilot project began, Sedron Technologies implemented component upgrades to protect against climate extremes, drying bed retrofits to improve the fuel supply quality. In its first year in Dakar, the JOP processed an estimated 700 tons of fecal sludge and continues to run on a nearly daily basis (*Project Overview / Sedron Technologies*, n.d.). Our goal is to scale up the Janicki Omniprocessors to provide a population of 1,000,000 residents with adequate sanitation services. A basis of 1,000,000 people was selected because that is the population of Dakar that lacks adequate sanitation services, and their daily waste will be collected, treated, and transformed into valuable products that will drastically improve their quality of lives.

3. Previous Work

The JOP is described as a “decentralized waste treatment system that kills pathogens while recovering valuable resources from fecal sludge, biosolids, and other waste streams (*Project Overview / Sedron Technologies*, n.d.)”. The JOP makes responsible waste treatment economically viable opposed to it becoming a burden on society since it creates three useful products. Therefore, making the scale up and design of this project worth further analysis and simulation, thus seen in this report.

JOP technology is currently in use in a pilot plant in Dakar, Senegal. It operates at a scale serving 100,000-200,000 people (Sanders, 2018). In a survey of various cities in underserved regions, we concluded that a service population of 1 million people would be most optimal for the deployment of this technology. In Dakar alone, there are 1 million people who lack access to adequate sanitation services. There is a dearth of publicly-available information about the specifications of the process, so in our scale-up project, we also hope to determine optimal operating conditions based on good engineering practices.

We will also investigate whether the use of reverse osmosis (RO) during the water separation stage of the water treatment process is justifiable. RO will force water through a semipermeable membrane filled with small pores, allowing for selective separation processes. This method will be used to remove all dissolved impurities from the feed to purify the saturated water. While there are other separation technologies used in water treatment, RO technology is the most relevant to the JOP design because of the added complexity of the feed stream containing wet human waste which contains dissolved minerals and salts (Rose et al., 2015). We believe that RO processing will allow us to better scale up the process from the current conventional filtration system in the JOP pilot plant.

4. Discussion

4.1. Project Scale

The reactor for this process is a combustor which burns the dried biosolids, coming out of the dryer, in the presence of oxygen, thus creating fertilizing ash and stack gas. Our design basis will be based on the daily processing of one million people's waste and transforming it into the products of potable water, fertilizing ash, and electricity. For this project, we define daily processing as operating at steady state and fully putting through the process a volume equivalent to the waste generated by one million people. This basis was selected because it is the approximate population of Dakar that lacks adequate sanitation services, and their daily waste will be collected, treated, and transformed into valuable products that will raise the quality of their lives.

4.2. Reactor Equipment

For the combustion process, we will utilize a natural draft furnace. All fired heaters operate based on draft, pressure differential between flue gases in the heater and ambient gas. This type of heater is the simplest and most reliable since the air supply does not require blowers and is powered by natural convection. It uses suction to create negative pressure inside the heater and pulls ambient air through the burner and into the combustion area (Garg, 2004). A typical fire heater has three major components: radiant section where the input is in contact with the fire, convection section where convection occurs, and stack flow where many of the gases are normally vented out into the atmosphere (Selinidis, 2019). However, for our process, the stack

gas will be funneled into a heat exchanger to cool the gas stream and recover energy to heat the steam that will enter a steam engine for electricity production.

4.3. Modeling the Combustion Reactor in Aspen

We simulated our combustor's performance in Aspen Plus. The combustor model was executed using an RGIBBS reactor. RGIBBS minimizes the Gibbs Free Energy in the system without the need for stoichiometric data. This allows us to simplify the simulation process, requiring us only to input feedstock components and their expected combustion products rather than individual reactions. Additionally, due to the extremely fast kinetics of combustion, it was assumed that the conversion of the incoming dried solids stream into its combustion products would occur almost instantaneously in the reactor. As a result, kinetics were neglected for the purposes of modeling the reactor. The non-random two liquid (NRTL) equation of state was selected on the basis of advice for reactions that have both polar and soluble salt components (Carlson, 1996). Figure 4.3-1 below shows an Aspen block flow diagram of the reactor.

The necessary inputs for this model were the identities and mass flows (kg/hr) of the feed components, the identities of the expected combustion products for those components, the temperatures and pressures of the input and air streams, and the reactor pressure. Since human waste is produced daily, the facility will run at a 90% uptime, leading to approximately 8,000 hours annually.

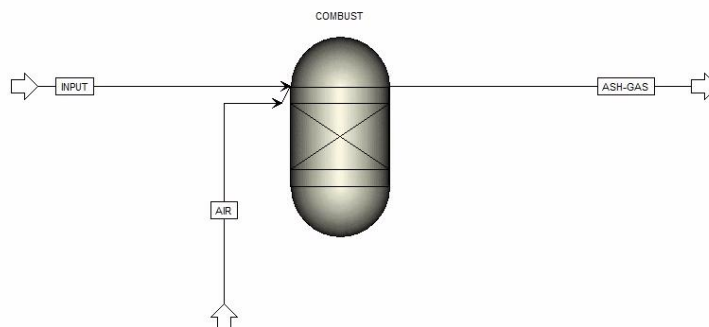


Figure 4.3-1. Block Flow Diagram of Reactor from Aspen Plus

4.4. Modeling Feedstock Components

The feedstock is modeled as a mixture of feces and urine. Elemental analyses were obtained for both feces and urine from data gathered and summarized by (Rose et al., 2015). The numbers provided were in terms of per capita daily generation, so the values were scaled up (by multiplying by a factor of 1,000,000) to represent a population of one million and units converted to kilograms, resulting in 1,680,000 kg of wet biosolids daily. Since the data presented by Rose et al. featured a review of contemporary sources (with some disagreement between numbers) in order to choose values for our feedstock, we aggregated the most recent values. In the situation where a range was provided, the average value was calculated and used. The complete dataset we compiled for a combined urine and feces stream is in Table C.4.4-1 in the Appendix.

An accurate simulation would feature all components present in the feedstock. However, it was impractical to input all of the components into Aspen Plus. Since many heavy metals were not present in the feed in large amounts, and were not expected to react appreciably, they were eliminated from simulation. However, heavy metal concentrations are critical for evaluating ash

quality and toxicity. As such, these heavy metals will be traced throughout our process, but not simulated in the combustion reaction.

Even after eliminating heavy metals, the remaining feedstock was still complex. After attempting to simulate the protein feed with four of the most common amino acids, it became apparent that the stock databases in Aspen do not have many of the organic compounds that are found in human feces. At this point, we considered using custom or biofuel input streams. However, performing the simulation in that manner would have required additional thermodynamic, kinetic, and stoichiometric data that we did not possess and could not find in literature. While there exists calorimetry for the burning of feces, there are few sources of the combined feed stream we are modeling (Yacob et al., 2018). As such, we decided to model the organic polymers in the feedstock as their respective monomers. We used the amino acid, lysine to represent protein, acetic acid for lipids/fatty acids, glucose for carbohydrates and fiber, and urea for major organic urine components. We originally planned to simulate our amino acids based on abundance found in literature, choosing the most abundant acids: alanine, glutamine, leucine, lysine, and valine (Bosch et al., 2018). Unfortunately, we could only utilize lysine as the other amino acids lacked thermodynamic data within Aspen. Acetic acid was chosen to represent fatty acids as healthy humans only produce short chain fatty acids in feces (Høverstad et al., 1984). Cellulose was originally chosen to represent fibers and undigested carbohydrates in our simulation based on literature review (Ho, n.d.). However, modeling cellulose would have necessitated more rigorous, biofuel-appropriate simulations. As such, we elected to simulate cellulose as its monomer, glucose, in order to continue usage of the RGIBBS reactor.

Additionally, literature on the composition of human feces did not provide enough specificity as to the chemical form of some of the elements and ions that were reported present in

feces. The typical elemental analyses found in literature were unrepresentative of the true oxidation states of many salts and ions found in the feedstock. Additionally, Aspen lacks data for many of the ions present in our system. To model the salts, we chose the salts present in the highest quantities. Since sodium was the most abundant cation while sulfate and phosphate were the most abundant anions, we modeled the salts using sodium sulfate and sodium phosphate, respectively (Rose et al., 2015). To convert the elemental composition by mass to these salt compositions by mass, stoichiometric conversions were performed based on the anions. Since the majority of phosphorus exists as phosphates in human waste, the mass of total phosphorus provided by Rose et al. was converted to the mass of total phosphates by molar mass ratio. The mass of sulfates was provided directly. The balance of sodium needed to complete the salt was then calculated and combined for the final values (Rose et al., 2015). Additionally, ammonia was omitted as a component as Aspen did not consider it compatible with sodium phosphate and sodium sulfate. Since the salts were larger fractions of the feed, we believe that greater accuracy of simulation could be achieved without the ammonia.

Even after the wet biosolids go into the dryer, we assume some unevaporated water is left in the solids. We assumed a value of 3,000 kg/day, or approximately 5% of the feed. Our air feed was represented by 21 mol% O₂ and 79 mol% N₂. Since it is a natural draft furnace, the air feed was simulated as coming in at ambient temperature and pressure (25°C and 1 atm) at a flow rate of 961,000 kg/day. With these design choices, our final simulated feedstock, our dry biosolids, to the reactor became as follows in Table 4.4-2.

Table 4.4-2. Simulated Feed Composition with Represented Components

Feed Component	Represented Component(s)	Daily Mass (kg/day)
Lysine	Protein (Amino Acids)	6,300
Acetic Acid	Lipids (Fatty Acids)	4,100
Glucose	Carbohydrates + Fiber	15,000
Urea	Urea, Creatine, Creatinine, Uric Acid	25,075
Sodium Sulfate	Sodium and Sulfate Ions	2,196
Sodium Phosphate	Sodium and Phosphate Ions	6,242
Water	Unevaporated Residual Water	3,000
Total		61,913

4.5. Furnace Simulation Results

In Aspen, the combustor specifications were set to be at 1 atm and zero heat duty ($Q = 0$). This resulted in a reactor temperature of 1570°C which is a relatively high value that will lead to most of our solid components vaporizing completely. In order to make the temperature suitable for heat exchanger use and to avoid a slagging reactor, diluent air was added until a reaction temperature of 600°C was achieved. By trial and error, we arrived at a flow rate of 961,000 kg/day of ambient air, simulated with a 21/79 ratio of oxygen to nitrogen gas. The exhaust gas composition is shown below in Table 4.5-1.

Table 4.5-1. Exhaust Components

Exhaust Component	Mass Flow (kg/day)
Oxygen	171,647
CO ₂	57,750
NO	6.5
NO ₂	1.2
N ₂	749,851
Water	34,938
Negligible amounts of CO, SO ₂ , SO ₃ , NaOH produced	

After running the simulation, the mass flow rates of the stack gas and fertilizing ash were determined through Aspen. These values are tabulated in Table C.4.5-1. The ash effluent has appreciable amounts of trisodium phosphate and sodium sulfate. It is also important to notice that the mass flow rates of sodium phosphate and sulfate salts influent are numerically identical to effluent. This is indicative of sodium salts not combusting into its expected products. Sodium phosphate represents an amalgamation of salts that are expected to exit in the ash product stream. In the stack gas, there are small amounts of NO_x, SO_x, and CO which will be addressed due to their risks to the health and safety of surrounding communities and the environment.

4.6. Steam Loop Simulation

After the exhaust gas is released from the furnace, the steam loop begins. Below, in Figure 4.6-1, is how the steam loop was modeled in Aspen using the method of IAPWS-95 in order to obtain temperatures, pressures, and heat duties for each unit operation. The basis for this

simulation was found in literature (*Simulation of Steam Engine with Aspen Plus V8.0*, 2012). The IAPWS-95 property set was chosen because steam is the only component of this system and the most accurate thermodynamic properties were desired.

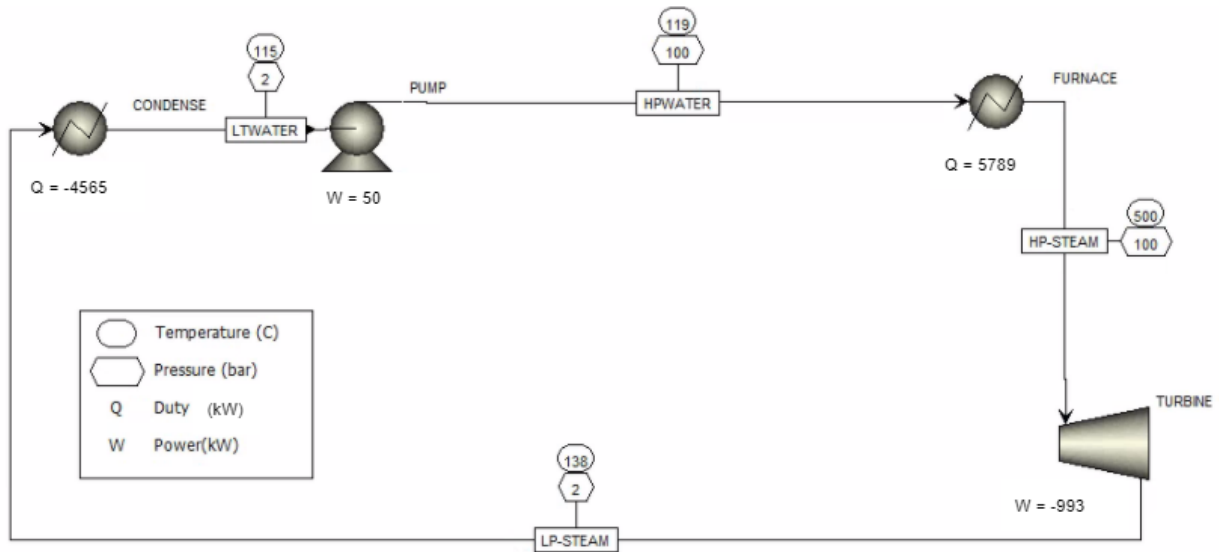


Figure 4.6-1. Steam Loop Simulation in Aspen Plus

The furnace was calculated to have an approximate heat duty of 6 megawatts (MW) from the previous combustion simulation. The high pressure water feeds into the furnace at 100 bar and 119°C and is then superheated to 500°C for feeding into the turbine. We chose this inlet temperature because the typical MOC (materials of construction) of turbines will usually only allow steam up to around 550°C (*Dresser-Rand Steam Turbines - a Siemens Business*, n.d.). The steam is then fed into the turbine which was designed to have a pressure drop of 98 bar, since a large pressure drop will allow more energy to operate the turbine. Aspen computed a temperature drop down to 138°C to accompany the pressure drop. The turbine produces 993 kW of power with an assumption that it is operating at a typical value of 78% efficiency (Peters et al., 2003). Typical turbine specs have a maximum of 550°C and 125 bar, therefore the operating specs were

lowered to avoid the upper limit. In order to get the full simulation, the steam being flown through the loop was determined starting from the furnace.

This steam flow rate was determined by finding the enthalpies of the exhaust stream and steam stream. The exhaust released from the furnace was modeled in Aspen using NRTL with components that did not have negligible amounts in the furnace (table 4.5-1). NRTL was chosen since there were polar gaseous components in our stream (Carlson, 1996)

The total flow rate was 40,750 kmol/day of exhaust gas, which for our flow rate shown in Table 4.6-1, amounted to a furnace heat duty of 520,028,247 kJ/day, or 6MW. The temperatures were chosen to provide a large temperature gradient for the exhaust gas (600°C to 200°C) and the steam (500°C and 119°C) for the heat exchanger. The temperature profile is shown below in Figure 4.6-2 and indicates that the second law of thermodynamics is not violated. For the steam, IAPWS-95 property sets were used to calculate the enthalpy difference between 100 bar steam at 119°C and 500°C. It was determined that 174,400 kg steam per day was to be fed throughout the steam loop through trial and error in Aspen. Trial and error was performed until the temperature profile fit our specifications and the temperature profile below. The ash stream chemical composition is shown below in Table 4.6-2. Since both sodium salts have melting points above 600°C they will both stay solid, and we will not have to deal with slagging conditions in our furnace.

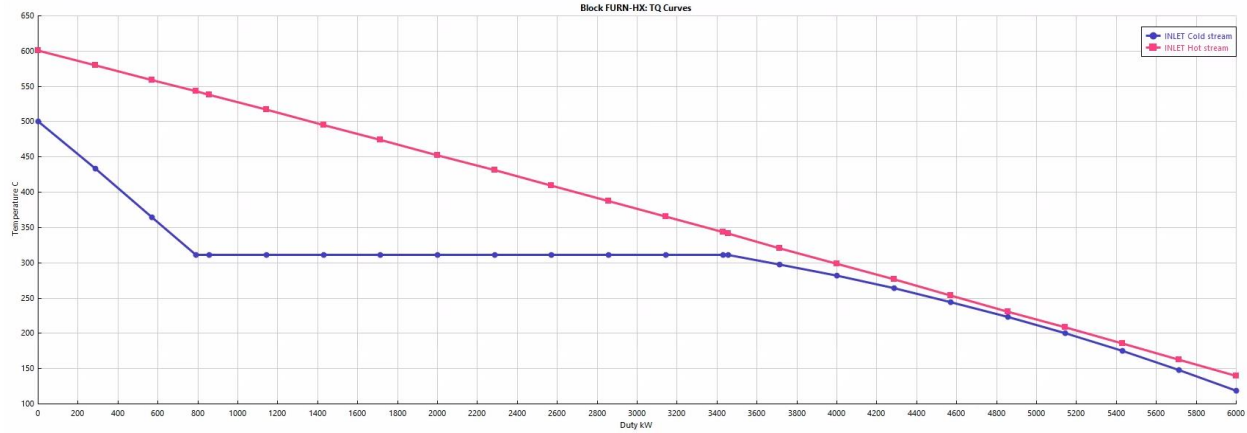


Figure 4.6-2. Temperature Profile for Furnace from Aspen

Table 4.6-2. Fertilizing Ash Components

Ash Component	Mass Flow (kg/day)
Na_2SO_4	2,196
Na_3PO_4	6,242

This steam leaving the turbine, now at a pressure of 2 bar, is then fed into a condenser to convert to liquid water. This phase change will provide a larger heat duty. This water is fed into the pump, working at a 42% efficiency, to pressurize it up to 100 bar and then fed into a preheater to vaporize the steam to be fed back into the furnace to finish off the loop. Another crucial flow rate was the sludge steam flow rate that leaves the dryer which would be fed to the separations part of the system. The dryer is powered by the condenser, and again the heat capacity of the input stream was simulated in Aspen with NRTL, on the basis of polar gaseous components. We calculated that the heat given off by the condenser could raise the temperature of the input stream from 25°C to 100°C and additionally vaporize 148,746 kg/day of sludge steam. The energy from condensing the steam is used to power the dryer and using that heat, that much of the wet biosolids can be evaporated. The full calculations are shown in Calculation

A.4.6-1 in the Appendix. The conditions for the dryer were chosen to be 1.5 bara, so that there was a positive pressure differential for pumping and 111°C, which is the temperature of vaporization of water at 1.5 bara. Available literature shows that the dryer is run at 100°C and 4 bar in Janicki's Omniprocessor, however, we were unable to simulate sufficient evaporation at those conditions (Janicki, n.d.-b). This indicates to us that the physical properties of the system require further investigation and practical experimentation, which are not available to us.

The amount of sludge steam vaporized, which is the amount of water we can separate from the wet biosolids stream, is 148,746 kg/day (Calculation A.4.6-1 in the Appendix). We will perform this separation in a dryer, consisting of a heat exchanger between the steam loop and the incoming biosolids, and a subsequent vapor-liquid separator. In the absence of physical properties and knowledge of pilot plant implementation, we did not perform heat exchanger or vapor/liquid separation simulations. We did, however, confirm that this was thermodynamically possible in our calculations. A good target for future work would be to collect physical data and characterize the vapor-liquid separation so that a practical dryer design can be chosen.

Based on our previous calculations, a population of 1 million humans will produce wet biosolids that contain 1,618,000 kg/day of water. As such, we will need to pass the wet biosolids through drying ponds first to remove a large portion of the liquid water from the input stream so that our dryer can feed adequately dry material into the furnace for combustion.

4.7. Separations and Water Purification Simulation

While the dried solids are being sent to the furnace, the sludge steam coming off the feedstock and out of the dryer enters the separations section of the process. The only useful product of the overall separation process is clean drinking water. Of the many feedstock

components coming into the dryer, only some of the components will be vaporized by the dryer conditions and go through the separation processes. As shown in Table 4.7-1, the components were chosen based on vapor pressures at 25°C. If the component had a similar or higher vapor pressure than water, then it was considered volatile enough to vaporize in the dryer and thus was chosen for modelling the components entering the separations process. Table 4.7-1 shows that only ammonia, creatinine, and uric acid met this criterion. To simplify the model further, the smallest component, ammonia, was chosen to represent these three components. This decision was based on the design specification that the separation processes will filter out any compound bigger than that smallest component. Since the dryer is heating up feces, there will be trace amounts of very small particulate matter that gets carried up with the volatile components. Thus, the sludge steam coming out of the dryer will be modelled as a mixture of water vapor, ammonia, and trace solid particulate matter. This sludge stream composition will come out of the dryer and enter the first separation process, the cyclone separator.

The cyclone separator, pictured below in Figure 4.7-1 can separate gas or vapor from particulates in that stream. It does not require a filter that would need to be cleaned during maintenance. Rather, particulate matter is removed from the vapor stream by forcing it toward the bottom of the cyclone separator. As particulate matter collects, it will be manually collected, removed, and placed back into the feedstock stream to reenter the dryer.

Table 4.7-1 Volatile Feed Components

Compound	Liquid Vapor Pressure at 25 °C (atm)	Volatile?	Amount in influent (kg/h)
Water	0.0313	Yes	14,921
Ammonia	9.87	Yes	25
Creatinine	0.2	Yes	--
Acetic Acid	0.024	Yes	--
Creatine	2.34×10^{-6}	No	--
Urea	1.58×10^{-8}	No	--

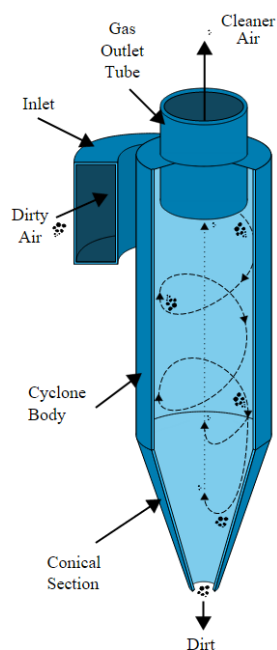


Figure 4.7-1. Cyclone Separator Cross Section Showing Generalized Air/Vapor Flow Patterns
(Afework et al., 2018)

This cyclone separator was assumed to have a diameter of 1.5 meters which is a typical value for an industrial cyclone separator. Dimensionless values for other design specifications

for the cyclone separator developed by Lapple (1951) were used to fully specify the size of the cyclone separator as shown in Table C.4.7-1 and Figure C.4.7-1 of the Appendix (Lapple, 1951). In order to find the efficiency of the cyclone, the particle density of one particle is assumed to be the same as that of fecal matter. Using these assumptions, we calculated d_{pc} , the particle size that can be removed at 50% efficiency and d_p , the size particle that can be removed at 100% efficiency. All particles 806 μm and larger can be removed 100% of the time and all particles of 570 μm and larger can be removed at 50% efficiency. From these values, the efficiency, η_j , to remove roughly any size was approximately 66.7%. Calculations of efficiency and particle diameters are in Calculation A.4.7-1 in the Appendix. An overall efficiency was not obtained because the total mass of particulates that are evaporating is unknown, therefore a lack of data hindered finding this value.

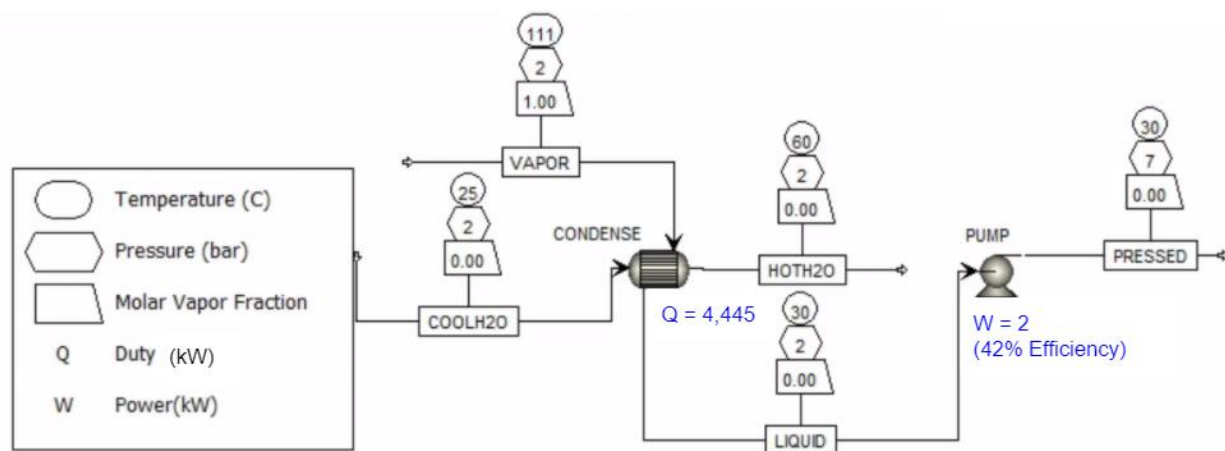


Figure 4.7-2. Aspen Plus Simulation of Condenser and Pump Before Reverse Osmosis

The condenser and pump were modeled in Aspen to obtain heat duties and amount of ammonium in the water flow rate, shown below in Figure 4.7-2. The particulate-free vapor leaving the cyclone is fed into the condenser which condenses the vapor and decreases the temperature of the stream from 111°C to 30°C. The value of 30°C was chosen in order to pass

the water through the RO system without damaging the polymer membranes. It was determined by a trial-and-error process, in Aspen, that close to 1,600,000 kg/day of cooling water at 25°C is required to meet this specification. The cooling water temperature coming out of the condenser is 60°C. A TQ Curve for the condenser is shown below in Figure 4.7-3 which demonstrates that these condenser conditions are feasible thermodynamically. The condenser operates at 1.5 bara and requires approximately 4,445 kW (Figure 4.7-2).

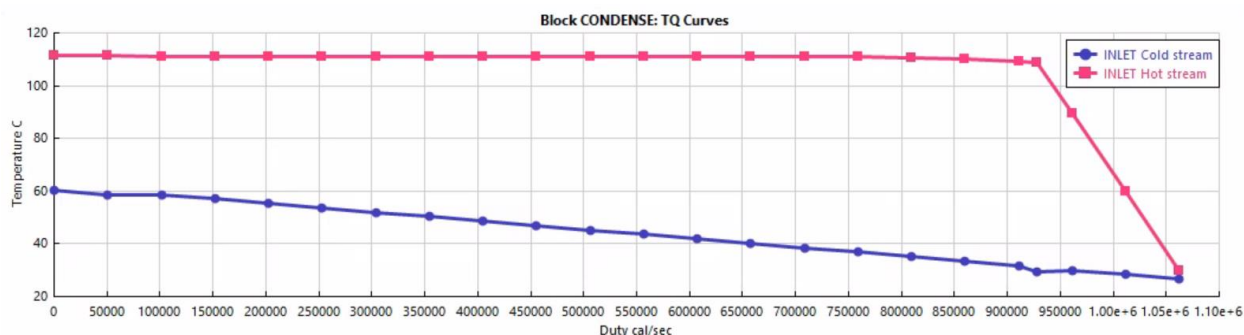


Figure 4.7-3. Temperature Profile for the Separations Condenser from Aspen

Before it flows through reverse osmosis (RO), the water pressure must be increased to 6.51 bara using a pump to overcome the natural osmotic pressure of the stream and force the water through the membrane. The pump has a specified efficiency of 42% and requires 2 kW of energy to operate.

Reverse osmosis (RO) is a pressure-driven membrane process used to remove a large majority of contaminants from water by pushing the water under pressure through a semipermeable membrane (Puretec Industrial Water, 2021). The semipermeable membrane allows minute molecules and ions to pass through it but acts as a barrier to larger molecules or dissolved substances (Toray Industries, Inc., 2021). Figure 4.7-4 below visually depicts a spiral-wound RO module and how it operates.

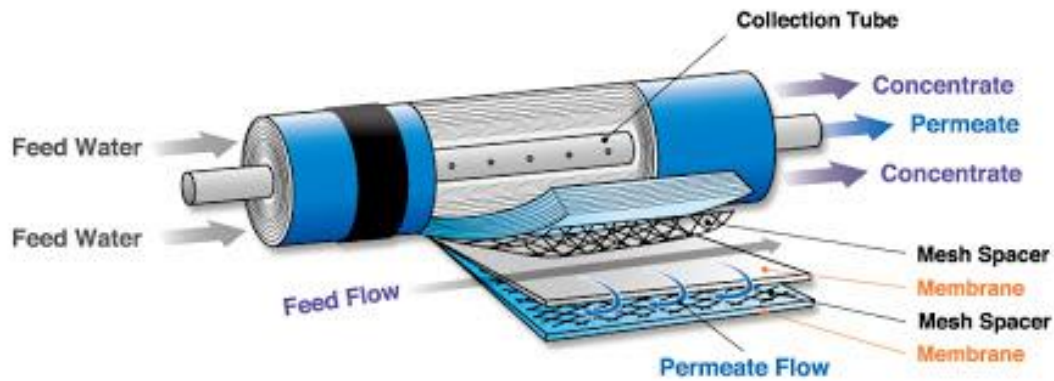


Figure 4.7-4. A Spiral Wound Reverse Osmosis Module (Aquanext, 2021)

From Figure 4.7-4, a specified number of membranes are wrapped around a central collection tube. The exact number of membranes needed is dependent on the nature of the feed water and desired level of separation. Each membrane is separated by mesh or feed spacers, which affect flux, pressure losses, and fouling in the membrane process (Boegger, n.d.). Unpurified feed water flows into the module from outside of the collection tube and cross flows radially into this central pipe. Along the water's path, it travels through the membranes, leaving behind trapped ions and other undesirable contaminants. Water that reaches the center collection pipe has been significantly treated to the desired purity. The purified water (permeate flow) exits out of the central gray collection tube in the permeate flow (Figure 4.7-4). The concentrate contains all of the material removed from the water and exits outside of the central gray tube to be properly treated and disposed of. This way, the permeate and concentrate flow exit in separated streams. This spiral wound RO module is the same mechanism that we will use in the simulation of the JOP RO process and it is assumed that it will operate by the above-mentioned process.

Important characteristics for designing an RO process include osmotic pressure, driving pressure, and salt passage/rejection. Osmotic pressure is defined as the minimum pressure that must be applied to the water solution side (feed water) to prevent the inward flow of the pure solvent side (permeate flow) across the semipermeable membrane (Feher, 2017; Wikimedia Foundation, 2021). Net driving pressure (NPD) refers to the difference between the feed water pressure and osmotic pressure (RO Chemicals, 2018). The NPD is the measure of the actual driving pressure available to force the water through the membrane (RO Chemicals, 2018). Purity is specified by a percent salt rejection and salt passage percentage. Rejection refers to the percentage of incoming contaminants that are withheld by the membranes and is rejected from exiting with the permeate flow. Passage refers to the percentage of original contaminants that are not withheld by the membranes and successfully exit in the permeate flow. Membrane type and membrane pore size are varied in order to achieve different salt rejection and passage percentages. The characteristics of the feed water and desired level of purity ultimately determine osmotic and driving pressures as well as salt rejection/passage percentages (Geise, 2008).

In order to simulate the RO process in the JOP, a Nitto Group Company program called "Hydranautics" was utilized. After our cyclone has removed particulate matter from the sludge steam exiting the initial dryer, it is condensed to water. For the purpose of our simulation, this water was assumed to only contain water and ammonia. However, the program automatically calculates the amount of ammonia present in water only when an input concentration of ammonium ions is given. Using ELECNRTL on Aspen, water and ammonia were simulated as the only two components entering the condenser. This was done to explicitly determine the mass flow rate of ammonium ions, partition in the condensed water. The mass flow rate of aqueous

ammonium was found in Aspen to be approximately 0.225 kg/h and the total volume flow rate was reported as approximately 104.3 L/min. After the conversion of units to share the same time unit and kg was converted to a more reasonable unit (mg), the mass flow rate of ammonium was divided by the total volume flow rate to determine its concentration that is expected to enter the RO process. This concentration of total dissolved ammonium, that was eventually entered into Hydranautics, was approximately 36.0 mg ammonium/L feed water (mg/L or ppm). Hydranautics used bicarbonate (HCO_3^-) as the default anion to balance this amount of cation as well as account for specified pH of the feed water. This balance concentration was approximately 121.8 mg HCO_3^- / L feed water. The feed stream had an assumed pH of 6.64 as this is the average pH of human waste (Rose et al., 2015). Figure 4.7-5 below shows the inputs (white boxes) and Hydranautics auto-calculations (grey boxes) to simulate the incoming feed stream. After specifying these inputs, Hydranautics auto-calculated the incoming concentration of ammonia to be approximately 0.09 mg/L. The total dissolved solids (TDS) in the feed stream were automatically calculated to be approximately 158 mg/L. The temperature of the feed water was specified as the temperature of water exiting the condenser (25°C) and the water type was denoted as “Municipal Waste” because this most closely resembled where the origin of JOP water.

pH	6.64	CO3	0.126 mg/l	CO2	30.008 mg/l	NH3	0.09 mg/l
----	------	-----	------------	-----	-------------	-----	-----------

Cations			Anions		
	mg/l	mg/l CaCO3		mg/l	mg/l CaCO3
Ca	0.00	0.00	HCO3	121.79	99.83
Mg	0.00	0.00	SO4	0.00	0.00
Na	0.00	0.00	Cl	0.00	0.00
K	0.00	0.00	F	0.00	0.00
NH4	36.00	99.83	NO3	0.00	0.00
Ba	0.000	0.00	PO4	0.00	0.00
Sr	0.000	0.00	SiO2	0.00	
			B	0.00	
Total, meq/l		2.00	Total, meq/l		2.00

Saturation				
Calculated TDS	158	mg/l	CaSO4	0.0 %
Osmotic pressure	0.1	bar	BaSO4	0.0 %
Ca3(PO4)2 SI	0.00		SrSO4	0.0 %
CCPP	0.00	mg/l CaCO3	CaF2	0.0 %
LSI	0.0		SiO2	0.0 %

Figure 4.7-5. Hydranautics Inputs for Feed Water Stream (Nitto Group Company, 2021)

Train Information		Pass 1	Pass 1	
Feed pH		6.64	Chemical	None
Permeate recovery	%	90.00	Chemical concentration	100
Permeate flow	m3/h	5.63	Chemical dose	0
Average flux	lmh	13.5	Membrane age	0.0
Feed flow	m3/h	6.26	Flux decline	15.0
Concentrate flow	m3/h	0.63	Fouling factor	1.00
			SP increase % per year	12.0

Figure 4.7-6. Hydranautics Specifications for Permeate and Concentrate Streams (Nitto Group Company, 2021)

Additionally, specifications were required in Hydranautics regarding the permeate flow and are shown in Figure 4.7-6 above. The incoming water mass flow rate was assumed to be the total volume flow rate from the Aspen simulation (104.3 L/min). This was converted to the units that Hydranautics provided (6.26 m³/h). The permeate flow (potable water flow) was simulated under the assumption of a 90% permeate recovery per the advice of Professor Geise. Therefore, the permeate flow was inputted as 90% of the incoming 6.26 m³/h of unpurified water (5.63 m³/h). The fouling factor was left at the default value of 1.00 because the Hydranautics stream is a simplified version of our actual feed and appreciable fouling behavior is not anticipated. It was assumed that the membrane age was 0 years as it was designed shortly before the time of this JOP process begins. From all of these assumptions and calculations, the concentrate flow was automatically determined by Hydranautics to be approximately 0.63 m³/h. All of the specifications for the outgoing permeate and concentrate streams can be seen in Figure 4.7-6

The recommended membrane type from Hydranautics, LFC3-LD-4040, was selected as this was advertised as the typical mechanism used for brackish water and “low pressure, high rejection” systems. After running the Hydranautics simulation, we developed a flow diagram (Figure 4.7-7 below) that displays the volumetric flow rate, TDS concentration, and pH for the three major streams. Additionally, it shows that the pump increases the pressure of the water leaving the condenser (at 0 barg or 1.01 bara) to 6.51 bara (5.5 barg). 6.51 bara represents the pressure necessary for forcing the water through each membrane. The feed flow contains 158 mg/L TDS and flows at the specified conditions (6.26 m³/h at a pH of 6.64). The undesired concentrate stream contains 1514 mg/L TDS and flows at approximately 10% of the incoming feed flow rate (0.623 m³/h). After the conversion of units, concentrate is flowing at

approximately 14,950 L/day. This stream is slightly more basic (pH = 7.58) than the incoming feed stream. Assumingly, this is because ammonia (a weak base) is being removed from the

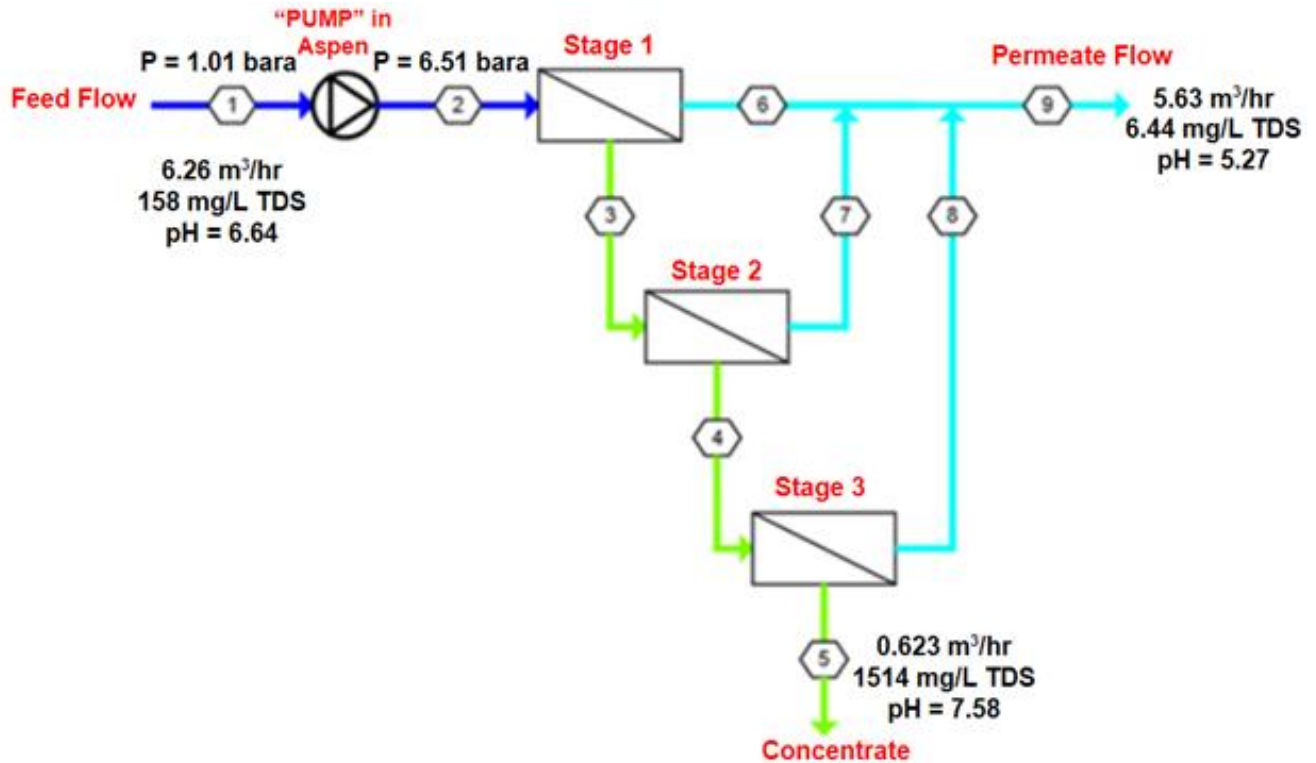


Figure 4.7-7. Hydranautics Reverse Osmosis Flow Diagram (Nitto Group Company, 2021)

water and dominates the concentrate stream. The permeate flow does flow at approximately 90% of the feed flow (5.63 m³/hr) with a substantially lower TDS concentration (6.44 mg/L TDS). From this information, the calculated salt rejection is approximately 95.9%. The approximate salt passage percentage is the balance, equating to 4.1%. The permeate flow is now purified, potable water. When converted from units of m³/hr to L/day, it was calculated that approximately 135,000 L/day of potable water is produced. This is indicative of the LFC3-LD-4040 membranes successfully withholding the dissolved ammonia and ammonium ions from entering the inner tube collecting purified water. The pH of the potable water is slightly more acidic than the feed flow (pH = 5.27). The typical pH range for drinking water is within 6.5-8.5 (Fawell, 2007).

Additionally, the US EPA has promulgated a secondary drinking water regulation pH in this same range (United States Environmental Protection Agency Office of Water, 2018). Therefore, an agent must be chosen and added to the water to raise the pH by more than 1.0 pH unit. This will be considered out-of-scope of our project. Figure 4.7-8 below provides a summary table provided by Hydranautics of all characteristics (flow (m³/h), pressure (barg), TDS concentration (mg/L), and pH) of the 9 streams in the RO process.

	1	2	3	4	5	6	7	8	9
Flow (m ³ /h)	6.26	6.26	2.99	1.65	0.623	3.27	1.34	1.02	5.63
Pressure (bar)	0	5.50	4.78	4.08	3.83	0	0	0	0
TDS (mg/l)	158	158	326	587	1514	3.05	5.73	18.1	6.44
pH	6.64	6.64	6.95	7.19	7.58	4.95	5.23	5.71	5.27
Econd (μS/cm) (@ 25.0 °C)	239	239	493	889	2169	8.50	10.3	28.9	11.6

Figure 4.7-8. Hydranautics Stream Table Summary (Nitto Group Company, 2021)

Permeate Concentration									
Ca	0.000	K	0.000	Sr	0.000	Cl	0.000	PO4	0.000
Mg	0.000	NH4	1.469	HCO3	4.970	NO3	0.000	SiO2	0.000
Na	0.000	Ba	0.000	SO4	0.000	F	0.000	B	0.000
								pH	5.3
								TDS	6.44 mg/l
Concentrate Saturations and Parameters									
CaSO4, %	0	SrSO4, %	0	Osmotic pressure	1.1 bar	pH	7.6		
BaSO4, %	0	SiO2, %	0	CCPP	0 mg/l	TDS	1514.4 mg/l		
Ca3(PO4)2 SI	0.00	CaF2, %	0	Langelier	0.00				

Figure 4.7-9. Cation/Anion Results for Permeate and Concentrate Streams (Nitto Group Company, 2021)

The osmotic pressure was calculated by Hydranautics to be 1.1 bar shown in Figure 4.7-9. Therefore, the driving pressure was found as the difference between 6.51 bara and 1.1 bara:

5.41 bara. Specific results were provided by Hydranautics in terms of ammonium and bicarbonate exiting in the permeate and concentrate streams (Figure 4.7-9). It can be seen that of the 6.44 mg/L TDS exiting in the permeate stream, approximately 1.47 mg/L is ammonium and 4.97 mg/L is bicarbonate. The National Academy of Science recommends, and many European nations have adopted, a drinking water standard of 0.5 ppm (Oregon Department of Human Services, 2000). The US EPA has established a life-time exposure advisory of 30 ppm for ammonia (Oregon Department of Human Services, 2000; United States Environmental Protection Agency Office of Water, 2018). Because the concentration of ammonium in the potable water stream is extremely diminished, it is assumed that dissolved ammonia was also effectively removed and only trace concentration remained. According to the US EPA, the national secondary drinking water standard for TDS is 500 ppm (United States Environmental Protection Agency Office of Water, 2015). In terms of ammonia and TDS, Hydranautics results show that the potable water was effectively treated within US EPA standards. However, pH adjustment would need to occur to meet US EPA secondary standards. According to Professor Mills, the pH of water could be raised by adding sodium bicarbonate (NaHCO_3) or sodium carbonate (Na_2CO_3) to the permeate stream leaving the RO process. Additionally, the addition of NaOH to this stream is a widely-used solution to low-pH water. The actual amount of agent needed to be added will not be calculated. However, pH adjustment is acknowledged as a necessary step in order to deliver this product as water treated to US EPA drinking water standards. Lastly, possible disinfection steps could be taken after the RO process to ensure that this water is devoid of pathogenic bacteria and safe for human consumption. Primary methods for drinking water disinfection may include chlorination, ozone, ultraviolet (UV) light, and

chloramines (Ishaq et al., 2018). In addition to pH adjustment, possible disinfection steps will be considered out-of-scope to the capstone project.

Hydranautics recommends three stages of RO treatment to achieve the desired purity in the permeate. Each RO stage (1-3) will require 7 LFC3-LD-4040 composite polyamide membrane elements. Hydranautics provides dimensions of each membrane element, which is shown in Figure 4.7-10 below. The LFC3-LD-4040 “low fouling spiral wound” configuration has an active membrane area of 80 ft² (7.43 m²) and feed spacer width of 34 mil (0.864 mm). The specified performance of each membrane element is 2,100 gpd (7.95 m³/d) and a salt rejection of 99.5-99.7%. The elements are 40 in long and 3.95 mm in diameter, with a core tube diameter of 1.05 in Figure 4.7-10.

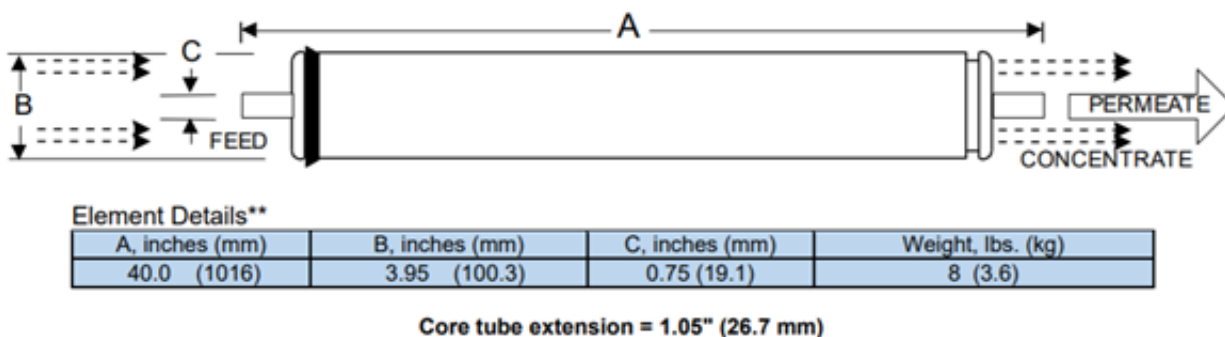


Figure 4.7-10. LFC3-LD-4040 Membrane Element Dimensions from Hydranautics (Nitto Group Company, 2021)

Stage 1 requires 4 vessels, while stages 2-3 require 2 vessels each. An example of a configuration for an RO pressure vessel is shown below in Figure 4.7-11 below. The vessel contains 7 membrane elements (similar to all RO membrane vessels in stages 1-3 of the RO process), each with different rejection and productivity levels. In the simulated RO process, stage 1 would contain 4 of these RO membrane vessels (and 28 membrane elements total). Stage 2 and

3 would contain 2 of these vessels (and 14 membrane elements). The RO vessels in each stage are in parallel to each other. After all 3 stages of RO, the final concentrate (stream 5 in Figure 4.7-7) and permeate stream (stream 9 in Figure 4.7-7) have been effectively separated. Purified potable water has been extracted from the JOP water separation process.

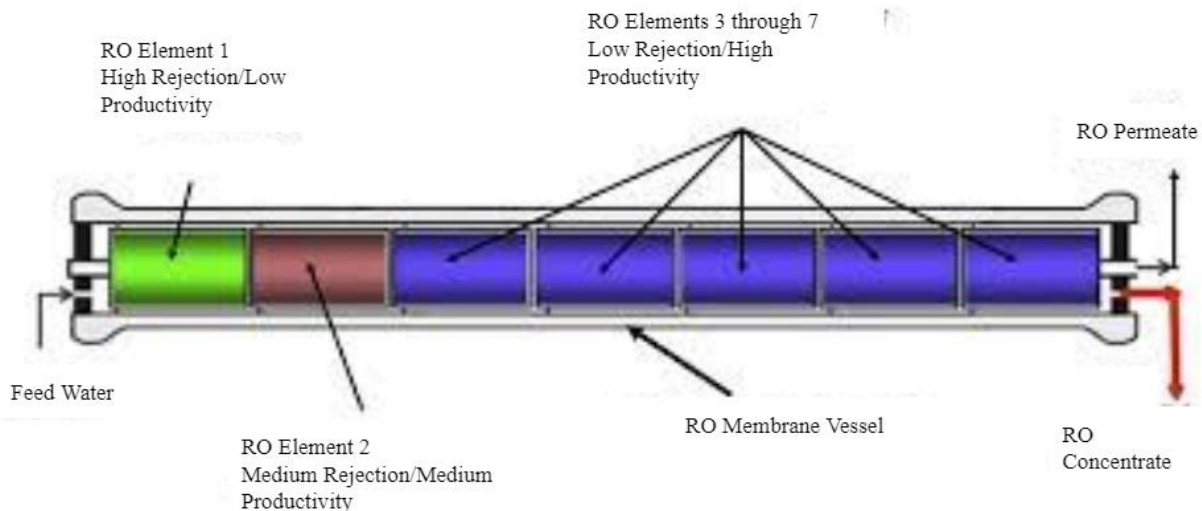


Figure 4.7-11. RO Membrane Vessel with 7 Membrane Elements (Korsen21, n.d.)

Backwashing will be utilized to clean the filter membranes by reversing the flow of water to remove any contaminant build-up on the membranes (Linerworld, 2009). This will serve as a preventative maintenance measure so that the filter media can be reused and debris does not disrupt desired passage/rejection levels. The volume of water and associated cost required for this process to occur is considered out-of-scope of this design because minimal fouling is expected. However, over time, backwashing is the necessary step to ensure proper maintenance and cleaning of the RO membranes. Additionally, to manage the RO concentrate that is separated from the potable water stream, typical sludge treatment processes will be implemented so the unwanted solids can be redirected to land application uses or the drying ponds (Filtration + Separation, 2021).

4.8. Drying Ponds

Since our condenser is only able to produce 148,000 kg/day of sludge steam, compared to a water mass of 1,168,000 kg/day, we will require drying ponds prior to the beginning of our process in order to evaporate the water that we cannot vaporize in the JOP. We used the EPA Evaporation equation, shown in Equation B.4.8-1 in the Appendix, which was developed to estimate evaporation from the surface of a pool of liquid that is at or near ambient temperature (Wanamaker, 2019).

We are determining the required drying pond surface area (A) in this equation, requiring a change in the unknown variable. The wind speed was determined to be 8.3 mph as the worst case scenario from data in Dakar (*Average Weather in Dakar, Senegal, Year Round - Weather Spark*, n.d.). The water's vapor pressure at 77.6°F (the average yearly temperature in Senegal) is 22.3 mm Hg (*Water Vapor Pressure Chart*, n.d.). The evaporation rate is 1,470,000 kg/day from the mass balance at the drying ponds which converts to 388,375 gallons/day. Based on these estimates, we determine that 10.44 acres of drying ponds are necessary, and the calculations are shown in Calculation A.4.8-2 of the Appendix. However, we have allowed a total of 14 acres for drying ponds, an extra 3.56 acres to account for any additional land for walkways, maintenance buildings, etc. Although we had hoped to generate enough heat to completely evaporate the moisture from our wet biosolids feed, the need for drying ponds is not a disappointment since the current pilot plant has similar requirements.

5. Final Recommended Design

A block flow diagram is shown below of our final process in Figure 5-1 below. Moisture will first be evaporating off of wet biosolids in drying ponds at a rate of 1,470,000 kg/day. The partially-dried biosolids are then sent into the dryer unit. The dryer unit, operated at 1.5 bara, uses heat from the condensation (in E-101) of steam in the steam loop in order to raise the temperature of biosolids to 111°C to vaporize the vast majority of the moisture left in the biosolids stream, 149,000 kg/day. In the vapor-liquid separator (V-101), the sludge steam and 30 dried biosolids separate. The sludge steam is then fed into a cyclone separator (DC-101) which separates the particulate solids from the vapor. The particulate solids are then mixed back into the dried solids stream. The vapor, still at 1.5 bara and 111°C, is condensed (in E-102) into liquid water and cooled to 30°C, and then pressurized in a pump (P-101) to 6.5 bara, the feed pressure required for the RO membrane system. After going through RO, the water is completely clean of all dissolved compounds and is completely potable. The dried solids stream is fed into a furnace (H-101) at a rate of 61,300 kg/day. The furnace produces hot exhaust gases at 600°C and these gases are passed over an internal heat exchanger that provides the heat to vaporize and superheat 174,400 kg/day of water, already at 100 bar, to 500°C in the steam loop. The furnace also produces 8,440 kg/day of ash at this stage, which can be sold as fertilizer. The superheated steam is then fed into a turbine (T-101) to generate 24,000 kWh of electricity a day and the low pressure steam, now at 2 bar and 138°C, is then fed back into the dryer to be condensed into water. Prior to re-entering the furnace, the water is re-pressurized to 100 bar in pump P-102.

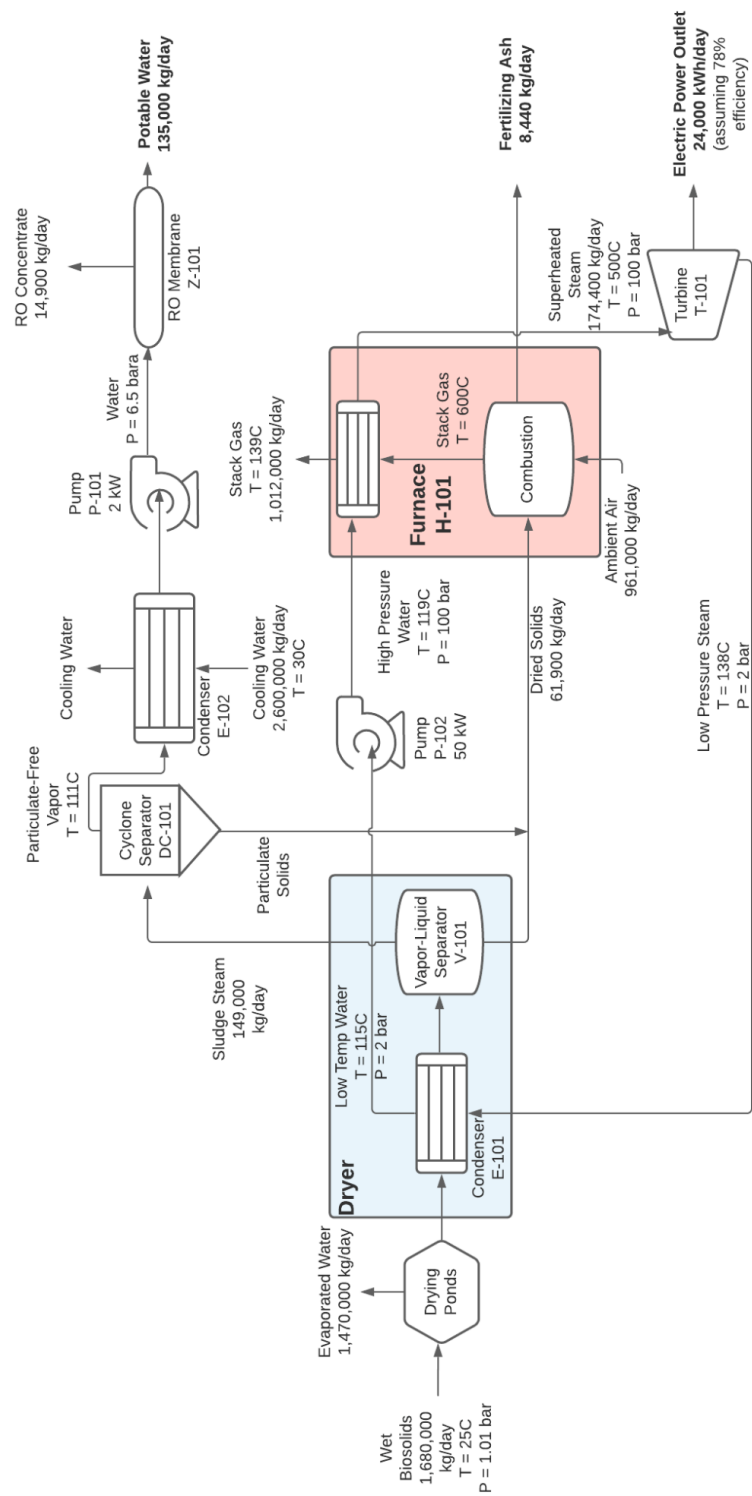


Figure 5-1. Overall Process Block Flow Diagram for JOP

The overall mass balance was organized into a table and the mass flow rates for the inputs (dry biosolids, water, and ambient air) and outputs (potable water, fertilizing ash, evaporated water, RO concentrate, and exhaust gas) are shown in Table 5-1 below. It can be seen that 60,000 kg/day of dry biosolids will create 8,440 kg/day of fertilizing ash. 1,620,000 kg/day of water will enter as a part of the wet waste and will result in 1,470,000 kg/day of evaporated water (in drying ponds), 135,000 kg/day of potable water, and 14,900 kg/day of RO concentrate. An input of 961,000 kg/day of ambient air inputted into the furnace will result in 1,012,000 kg/day of exhaust gas. The overall mass flow balances with approximately 2,640,000 kg/day of material flowing both in the process and out.

Table 5-1. Overall Mass Balance

Input (kg/day)	Output (kg/day)
60,000 Biosolids	8,440 Fertilizing Ash
1,620,000 Water (in Waste)	135,000 Potable water 1,470,000 Evaporated water 14,900 RO Concentrate
961,000 Ambient Air	1,012,000 Exhaust Gas

This JOP design requires the equipment shown in Table 5-2. These components were all priced using CAPCOST, and the purchased equipment costs are shown in the tables below (Turton, 2018). Given the high costs and reliability of the systems, we did not plan for duplicate purchases of any of our major equipment. Stainless steel construction was used for all equipment in order to avoid corrosion given the potential corrosive and fouling properties of our feed streams. The furnace was priced as a pyrolysis furnace with a heat duty of 20,800 MJ/hr. The turbine was priced as an axial turbine, generating 993 kW. Our steam loop condenser, which also

provides heat for the dryer, was priced as a heat exchanger and a vapor-liquid separator. While we have simulated our process using these unit operations, we are uncertain of the optimal implementation of a biosolid evaporation system, and would require further physical property data and practical experience to determine.

Table 5-2. Full Equipment for Entire Process

Equipment	Ancillary Equipment
<ul style="list-style-type: none"> ● Vapor-/Liquid Separator ● RO Pressure Vessels <ul style="list-style-type: none"> ○ RO Membranes ● Cyclone Separator ● Pyrolysis Furnace ● Turbine 	<ul style="list-style-type: none"> ● Storage Tanks (4) <ul style="list-style-type: none"> ○ Partially Dried Sludge ○ Potable Water ○ RO Concentrate ○ Fertilizing Ash ● Steam Loop Pump ● Reverse Osmosis Pump ● Furnace Heat Exchanger ● Dryer Heat Exchanger

The vapor-liquid separator was priced as a vessel. Given that we lack physical property data for actual vessel sizing requirements, we priced the separator as a vertical vessel, 5 meters in height, 2 meters in diameter, and capable of containing a pressure of 5 barg. In the absence of physical vapor-liquid separation data, a large size was chosen, with a slight pressure headroom to allow for expansion. The RO system was priced using provided information for a similar membrane vessel on Hydranautics. While the program did have the cost for the desired LFC3-LD-4040 series of membrane vessels, it was available for the CPA5-LD series. Both series are classified in Hydranautics "high rejection and brackish water thin film reverse osmosis membranes" and have identical 8'' x 40'' dimensions (WaterAnywhere, 2020). The CPA5-LD membrane vessel was estimated to cost \$693 per vessel. Each vessel was assumed to contain

seven membrane elements as the actual number of elements was not specified. A total of eight membrane vessels (in three total stages of RO) was specified by Hydranautics to adequately purify the water. Therefore, the total cost of the RO system was found to be approximately \$5,544, shown in Table 5-3, below. This value was directly inputted into CAPCOST as “user-added equipment”. Finally, the cyclone separator was priced as a cyclone dust collector capable of receiving 0.002 m³/s and was calculated to be approximately \$1,640, shown in Table 5-3.

Table 5-3. Equipment Costing

Equipment	Purchased Equipment Cost
Pyrolysis Furnace (H-101)	\$1,239,000
Turbine (T-101)	\$636,000
Vapor-Liquid Separator (V-101)	\$98,900
RO System	\$5,544
Cyclone Separator (DC-101)	\$1,640
Total Equipment Cost	\$1,981,084

In order to determine the sizes of the storage tanks, it was assumed that they would hold a week’s worth of material before emptying. We then sized the tanks at 1.5 times the weekly volume to prevent overfilling. The partially-dried sludge storage tank was designed to hold 1420m³ of material, the potable water tank 315m³, the RO concentrate tank 157m³, and the fertilizing ash tank, 35m³. Again, all tanks were constructed from stainless steel in order to prevent corrosion. The prices are shown below in Table 5-4. The two heat exchangers were priced as fixed exchangers also made of stainless steel. The dryer heat exchanger had an area of 112m² (obtained from Aspen), shell-side pressure of 0.99 barg, and tube-side pressure of 0.99

barg. The respective values for the separations heat exchanger were 96, 0.49, and 0.49. The pumps were priced as centrifugal, stainless steel pumps. The RO pump was specified to have a power load of 2.1 kW and a discharge pressure of 5.5 barg. For the steam loop pump, those same specifications were 50 and 99, respectively. Due to their low cost and mechanical complexity, we decided to purchase 1 spare for each of the pumps.

Table 5-4. Ancillary Equipment Costing

Equipment	Purchased Equipment Cost
Partially Dried Sludge Storage Tank	\$148,000
Steam Loop Pump (P-102) (1 spare)	\$128,000
Dryer Heat Exchanger (E-101)	\$91,500
Separations Heat Exchanger (E-102)	\$86,600
Potable Water Tank	\$78,600
RO Concentrate Tank	\$64,600
Fertilizing Ash Tank	\$57,700
RO Pump (P-101) (1 spare)	\$16,500
Total Ancillary Equipment Cost	\$671,500

The total equipment, calculated from adding both Table 5-3 and Table 5-4 prices, cost approximately 2,650,000 USD. To account for piping, instrumentation, land, and other discretionary costs, a Lang factor of 4.74 was used on CAPCOST — this totals to 12.6 million USD for the fixed capital investment. This factor was chosen as a default since our process is not expected to require special considerations. However, the land costs in the Lang Factor may be insufficient to cover the land necessary for the drying ponds. As such, we have allowed an additional 2,100,000 USD for 14 acres of land by using the average price of land in Thiès, a neighboring city to Dakar, as 62.67 USD for every 1 m² (“Where and How to Buy Land in Senegal,” 2020). The drying ponds would ultimately need more construction than simply digging into the ground. The price of land in the outskirts of Dakar is approximately 63 USD/m². Approximately 1 million USD was allocated to cover the cost of any site preparation for lining or concrete insertion. Incorporating the drying ponds and possible construction, the total value of our fixed capital investment for the plant is 15,700,000 USD. We recommend that we investigate technology to prevent leaching and mitigate odor issues from the sewage drying stage of the process.

In Senegal, 350,000 CFA/month is the median monthly salary in Senegal (Salary Explorer, 2021). This was used in order to determine the operating labor costs for the plant. After assuming 2,080 hours/year and determining 127 employees, the total payroll amount amounts to approximately 1.06 million USD per year, with the calculation shown in Calculation A.5-1 in the appendix (Turton, 2018).

The majority of the process is self-sustainable and provides much of the usual materials and utility costs on its own. However, in the separations process, external cooling water at 25°C is used in order to get the temperature of the particulate-free vapor entering the condenser down

to 30°C when it leaves. The cooling water is flown at a rate of 2,600,000 kg/day pricing at 15.7 USD per 1000m³; it costs 14,800 USD per year to provide this cooling water externally (Turton, 2018). Additionally, we will need boiler free water to refill the steam loop. We assumed that we would require 2% of the volume, so for the 174,400 kg of steam per day, it will cost just under 2,000 USD per year at \$1.523/1000 kg steam (Turton, 2018).

In terms of revenue, the process has three priced outputs: water, electricity, and fertilizing ash. The annual gross revenue per year would be approximately 4.06 million USD. The full breakdown of unit costs is expressed below in Table 5-5. Our process will be providing a sanitation system therefore, in capitalistic societies, we may be justified in charging for the use of our system. We will cost our stream as zero since our venture is philanthropic in nature. The cost of electricity today in Senegal is 0.184 USD/kWh (*Senegal Energy Prices / GlobalPetrolPrices.Com*, 2020). Sedron currently sells the water produced for 0.05 USD/L, which we plan to match, and ash at 20 USD/ton (Janicki, n.d.-a). Using these numbers, the revenue was calculated, and is shown in Table 5-5.

Table 5-5. Table of Revenue for Plant

Stream	Quantity (units/day)	Unit Cost (USD/units)	Cash Flow (USD/day)
Input Stream	1,680,000 kg	0.00	0
Water Output	135,000 L	0.05	6,750
Electricity Output	23,000 kWh	0.18	4,200
Ash Output	8,440 kg	0.02	169
Total Daily Revenue (USD/day)			\$11,100

Annual Gross Revenue (USD/year)	\$4,060,000
--	--------------------

A discounted cash flow analysis was performed after determining the fixed capital investment, costs, and revenue for the plant and can be seen below in Figure 5-2. We incorporated a tax rate of 40%, which is in reality the personal income tax rate in Senegal, while the corporate tax rate is 35% (Trading Economics, 2021). The 40% rate was used to have the worst-case scenario present in the analysis. With this tax rate, we achieved a current internal rate of return of 14.5% after a 20-year plant life-span and a 7-year straight-line depreciation — this value is high enough to justify investment. The capital expense in year -1 and 0 indicate the beginning of the plant without enough revenue generation. At year 1, The plant starts making profit with a depreciation cost of just under 2 million USD. At the 20th year, the net present value shoots higher than previous years since it accounts for the 14-acre land that would be expected to be sold back at the end of the plant life-span.

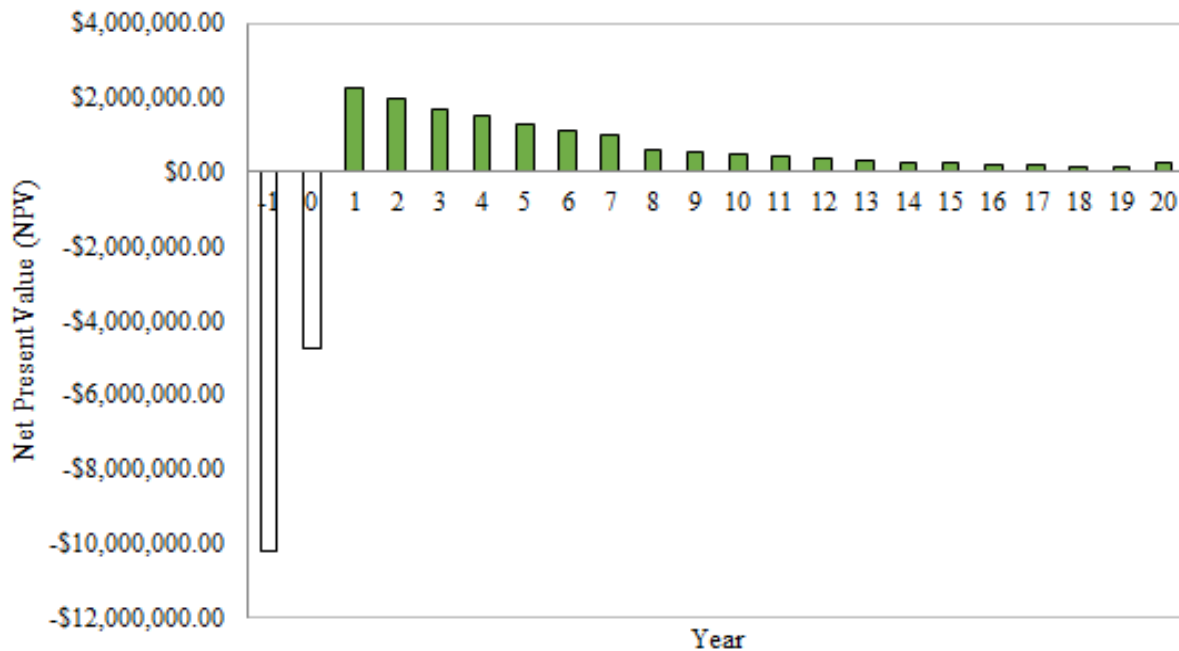


Figure 5-2. Annual Discounted Cash Flow

From this analysis, this plant project would be a profitable endeavor and can proceed with further investigation. Namely, we would recommend the collection of additional physical property data and chemical analysis and characterization of the actual waste streams. A better chemical analysis would allow for the optimization and better simulation of the furnace and steam loop, and better physical property data would allow for the proper design of the dryer. A true moisture content of the waste stream would also allow for a more precise decision making regarding drying ponds. These additional data would also enable more accurate characterizations of the fertilizing ash and provide a basis for optimizing the process.

6. Health and Environmental Safety

In the stack gas stream leaving the furnace, there are appreciable amounts of NO_x and SO_x : 6.5 kg NO /day, 1.2 kg NO_2 /day, 0.0028 kg SO_2 /day, and 0.013 kg SO_3 /day (Figure C.4.5-1). These compounds are vented into the atmosphere after entering a heat exchanger and, therefore, pose notable risks to human health, especially those in closest proximity to JOP operation (employees and neighboring communities). NO_x has been known to cause breathing problems, headaches, chronically reduced lung function, eye irritation, loss of appetite, and corroded teeth (Phys.org, 2015). Nitrogen oxides also pose environmental issues when emitted into the atmosphere. These gases act as indirect greenhouse gases by producing a tropospheric greenhouse gas, ozone, via photochemical reactions in the atmosphere (GHG Online, n.d.). Elevated exposures to ozone can affect sensitive vegetation during growing season and ecosystems, including forests, parks, wildlife refuges, and wilderness areas (United States Environmental Protection Agency, 2015a). Additionally, nitrogen oxides are involved in the creation of photochemical smog, which contributes to poorer air quality (Environmental Protection Authority, 2004).

High concentrations of SO_x can react with other chemicals in the air, lessen their particle size, and enter into the lungs (United States National Park Service, 2018). This gas can cause inflammation and irritation of the respiratory system, causing coughing, throat irritation, and breathing difficulties (United States National Park Service, 2018). These compounds can affect lung function, worsen asthma attacks, and worsen heart disease (United States National Park Service, 2018). SO_x compounds are also key air pollutants that can harm trees and plants by damaging foliage and decreasing growth (United States Environmental Protection Agency,

2016). SO₂ in particular contributes to acid rain, causing the erosion of buildings, damage of vegetation and soil, disruption of aquatic ecosystems, and reduced visibility.

A massive amount of CO₂ (57,750 kg/day) also vents into the atmosphere in the stack gas stream. Carbon dioxide makes up the vast majority of greenhouse gas emissions, roughly 80% in 2019 (United States Environmental Protection Agency, 2015b). These greenhouse gases trap heat within the atmosphere and contribute to the warming of the planet and accelerate climate change (United States Environmental Protection Agency, 2015b). To abate the amount of NO_x, SO_x, and CO₂ being directly released into the atmosphere from this design, greenhouse gas capturing technology should be strongly considered to mitigate the effects of these gases on the environment and humans.

14 acres of drying ponds containing feces poses threats to the surrounding environment and the health and quality of life of any nearby communities. Firstly, there will most likely be a severe odor for anybody removing the waste from the drying ponds or communities living within a few-mile radius of the site. To address this concern, odor mitigation techniques should be investigated so daily lives of communities and JOP employees are not harmed. Secondly, storing feces in the open atmosphere shows the risk of possible leaching of pathogens and/or chemical pollutants into the surrounding soil or surface and drinking water sources nearby. Feces-contaminated water is a vector of a plethora of human diseases, such as cholera, typhoid, hepatitis, polio, and cryptosporidiosis (Carr, 2001). At the very least, vaccinations against these diseases will be required for employees who will work in close proximity to disease-laden human waste. To mitigate the risk to surrounding communities, a flexible membrane liner (similar to one used in traditional landfills) should be placed between the drying pond and soil to act as an impermeable barrier. This liner is typically made of clay and prevents humans and the

environment from being exposed to the diseases and symptoms associated with direct exposure to feces.

It is anticipated that the water produced from the JOP process will meet all primary drinking water standards set by the United States Environmental Protection Agency (ammonia and TDS). While the potable water does not meet the US EPA's secondary drinking water standard for pH (6.5-8.5), it is not expected that this will have any sort of negative effect on the health of the consumer. However, pH adjustment steps (through the addition of sodium carbonate, sodium bicarbonate, or NaOH) may be required so consumers feel comfortable with the taste and aesthetic of the drinking water. Additionally, the "yuck factor" is an anticipated social barrier that refers to public reluctance to drink water derived from waste. However, this could be negligible in the context of Senegal because of the country's high percentage of people lacking access to the basic necessity in the first place.

The steam cycle, furnace, and turbines will also be operating at high temperatures (up to 600°C), high pressures (100 bar), and dangerous mechanical rotations. As such, proper care should be taken to insulate pipes, and instrumentation installed in order to prevent overheating or overpressurization. Precautions must also be taken around mechanical equipment to prevent injury or dismemberment. Additionally, depending on final furnace design, workers may be required to enter the furnace periodically to manually remove the ash. In this situation lock-out-tag-out, oxygen monitoring, smoke prevention, and cleanliness precautions and procedures should be developed and observed in the plant. Workers in the plant will need to be trained on these procedures and have secure risk-management knowledge.

7. Conclusion

Hundreds of millions of people around the world don't have clean water to drink and billions of people do not have access to proper sanitation services. In 2011, Sedron Technologies deployed the pilot scale JOP in Dakar, Senegal to simultaneously address these growing problems by taking the waste of people and generating clean drinking water and electricity. The goal of our project was to scale and specify this pilot project to serve 1,000,000 people with sanitation services and provide added drinking water, electricity, and fertilizing ash.

The scaled and specified process begins with drying ponds which were added to reduce the water content of the waste to optimize the system. Heavy metals and other elemental components that Aspen took issue with were excluded from modelling and simulation of the feedstock. It was simulated in Aspen as lysine, acetic acid, glucose, urea, sodium sulfate, sodium phosphate, and water, and inputted into the dryer unit. The vapor-liquid separator is a point of departure for the sludge steam floating upwards and the dried solids into the furnace. The dried solids are fed into the furnace and the combustion reaction produces stack gas containing several contaminants, but also 8,440 kg of fertilizing ash per day, one of the three major products. Relatively low temperature water is separated from the dried solids and converted to 174,400 kg of superheated steam which is used in the turbine per day which in turn generates 24,000 kWh of electricity per day, another product of the JOP. This superheated steam is fed into the condenser in the dryer to sustain the continuous steam loop. In order to produce the potable water, sludge steam from the vapor-liquid separator is input into a cyclone separator, which cleans the vapor of any significant particles, to begin the water condensing and purification process. External cooling water is fed through the condenser to obtain acceptable water temperature and pressure

for the reverse osmosis (RO). The RO membranes thoroughly purify the water to produce 135,000 kg every day, simulated in the Hydranautics program, and becomes the final product of the JOP process. This design with these specifications of each step of the process grants a reasonable and profitable plant which proves to be heavily useful for sanitation and drinking water purposes.

The human feces will be free as the process will become a service for the city, while the three products will have prices which will accumulate to over 4,000,000 USD every year for revenue and 7-year straight line depreciation. We achieved a current internal rate of return of 14.5% through a discounted cash flow analysis assuming a 20-year plant life-span. It is possible for the plant to be more profitable than calculated as the 40% tax rate was at the higher range displaying higher losses than it may actually be. Thus, the execution and investment of this JOP process are deemed profitable for future ventures. While the plant may have financial success, the service itself will be extremely helpful for the city of Dakar due to its waste disposal and sanitation services. This ultimately reduces the chances of spread of contamination and water-borne diseases, increasing the overall health, safety, and quality of life for the citizens of Dakar, Senegal.

We recommend that future work be completed to better characterize the waste stream. Without first-hand, local knowledge, we were unable to properly specify the waste feed stream's composition. Questions such as whether both urination and defecation occur in pit latrines, length of time that human waste remains in the latrines, sanitation practices, and latrine lining should be answered. This would allow for a better characterization of the moisture level as well as the chemical composition of the initial waste stream. This would affect the drying pond areas and furnace combustion properties. Fertilizing ash chemical composition will also be better

simulated with a more accurate characterization. Additionally, the physical properties of the waste stream also require better characterization. This would enable the optimization of the dryer and better design for the cyclone separator. For the RO system, future work could include expanding the list of components that were included on the Hydranautics program (beyond just ammonia) and running the simulation. This would result in a more accurate version of the RO system of membrane vessels. Additionally, optimizing the type of membrane vessel series in Hydranautics could maximize the amount of contaminant removal for the price of the vessel.

8. Acknowledgements

Throughout the writing of this report, we have received a great deal of support and assistance. Firstly, we would first like to thank our supervisor, Professor Anderson (UVA ChE Department), whose expertise was invaluable in formulating the research questions and methodology, with help in Aspen simulations and pinpointing issues in the design. The insightful feedback pushed us to sharpen our thinking and brought our work to a higher level. Additionally, we would like to acknowledge Professor Geise (UVA ChE Department) and Professor Mills (UVA EVSC Department) who assisted our team in this capstone project by meeting with us to provide important information for the process of achieving the project results.

9. Appendix

Appendix A. Calculations

Calculation A.4.6-1 for sludge steam vaporization

Q[Condenser] = 4,565 kW → *simulated on Aspen and shown in Figure 4.6-1*

Q[Dry Components] = 117.459 kW → *simulated on Aspen by NRTL @ 1.5 bar, 25°C to 111.349°C*

Q[Water] = Q[Condenser] - Q[Dry Components] = 4565 - 117.459 = 4447.5 kW

Q[Water/(kg/day)] = 0.0299 kW/(kg water/day) → *simulated on Aspen by IAPWS-95 @ 1.5 bar*

Amount of H₂O = 4,447.5/0.0299 = **148,746 kg sludge steam/day**

Calculation A.4.7-1. Cyclone Calculation (Lapple, 1951)

$$N = \frac{l}{H} (L_b + \frac{L_c}{2}) = \frac{l}{0.75 m} (3 m + \frac{3 m}{2}) = 6$$

$$V_i = \frac{Q}{WH} = \frac{0.00172 \frac{m^3}{s}}{0.375 m * 0.75 m} = 6.12 * 10^{-3} \frac{m}{s}$$

$$\begin{aligned} d_p &= \left(\frac{9\mu W}{\pi N V_i (\rho_p - \rho_a)} \right)^{1/2} = \left(\frac{9 * 0.0002221 \frac{kg}{m * s} * 0.375 m}{\pi * 6 * 0.00612 \frac{m}{s} * (1000 \frac{kg}{m^3} - 0.919 \frac{kg}{m^3})} \right)^{1/2} \\ &= 806 * 10^{-6} m \end{aligned}$$

$$\begin{aligned} d_{pc} &= \left(\frac{9\mu W}{2\pi N V_i (\rho_p - \rho_a)} \right)^{1/2} = \left(\frac{9 * 0.0002221 \frac{kg}{m * s} * 0.375 m}{2 * \pi * 6 * 0.00612 \frac{m}{s} * (1000 \frac{kg}{m^3} - 0.919 \frac{kg}{m^3})} \right)^{1/2} \\ &= 570 * 10^{-6} m \end{aligned}$$

$$\eta_j = \frac{l}{(1 + \frac{d_{pc}}{d_p})^2} = \frac{l}{(1 + \frac{570 * 10^{-6} m}{806 * 10^{-6} m})^2} = 0.66$$

where,

N = number of turns inside the device (no units)

W = width of inlet (m or ft)

H = height of inlet duct (m or ft)

L_b = length of cyclone body (m or ft)

L_c = length (vertical) of cyclone cone (m or ft)

V_i = gas inlet velocity (m/s or ft/s)

Q = volumetric inflow (m³/s or ft³/s)

d_p = diameter of particle collected with 100% efficiency (m or ft)

d_{pc} = diameter of particle collected with 50% efficiency (m or ft)

μ = air viscosity at 100 °C (kg/m · s)

ρ_p = density of particulate particle (kg/m³)

ρ_a = air density at 100 °C (kg/m³)

η_j = collection efficiency of particles in the jth size range (0 < j < 1)

Calculation A.4.8-2. Calculation for Minimum Drying Pond Area (Wanamaker, 2019)

$$A = \frac{E(T+459.67)}{7.4P(0.447W)^{0.78}} = \frac{388375 (77.6+459.67)}{7.4(22.3)(0.447*8.3)^{0.78}} = 454,764.4 \text{ ft}^2 = \mathbf{10.44 \text{ acres}}$$

Calculation A.5-1. Cost of Operating Labor (Turton, 2018)

$$1) N_{OL} = (6.29 + 31.7 P^2 + 0.23N_{np})^{0.5}$$

where N_{OL} is the number of operators per shift

P is the number of processing steps involving the handling of particulate solids

N_{np} is the number of nonparticulate processing steps and includes compression, heating and cooling, mixing, and reaction.

$$2) N_{np} = \sum \text{Equipment}$$

$$P = \text{cyclone} + \text{dryer} + \text{furnace} + \text{ash} + RO = 5$$

$$N_{np} = \text{condenser} + 2 \text{ pumps} + \text{drying ponds} + 2 \text{ HE} + \text{turbine} = 7$$

$$N_{OL} = (6.29 + 31.7 * 5^2 + 0.23 * 7)^{0.5} = 28.3 \text{ operators} * 4.5 = \mathbf{127 \text{ people}}$$

Appendix B. Equations

$$E = \frac{7.4PA(0.447W)^{0.78}}{T+459.67} \text{ where,}$$

A = Pool Surface Area (ft²)

W = Wind Speed Above Surface (mph)

P = Water's Vapor Pressure (mm Hg) at Ambient Temperature

T = Temperature (°F)

E = Evaporation Rate (gallons/day)

Equation B.4.8-1. Equation for Evaporation Rate (Wanamaker, 2019)

Appendix C. Tables of Data

Table C.4.4-1. Complete, Scaled Aggregate Data for Input Stream Components

Total Wet Weight	1,680,000
Total Dry Weight	62,700
Component	Daily mass (kg/day)
Protein (Bacterial + Human)	6,300
Lipids	4,100
Carbohydrates	9,000
Fiber (Cellulose)	6,000
Total Phosphorus	1,180
Total Potassium	2,340
Calcium	645
Sodium	4,790
Cadmium	1.26
Zinc	12
Mercury	0.007
Lead	0.0013
Copper	1.1
Iron	850
Manganese	57
Urea	22,500
Ammonia	600
Creatine	75

Creatinine	1,640
Uric Acid	860
Sulfate Ions	1,485
Magnesium	200

Table C.4.5-1. Tabular Form of Combustor Mass Balance

Mass Flows	Input (kg/day)	Air (kg/day)	Fertilizing Ash (kg/day)	Stack Gas (kg/day)
Water	3,000	0	0	34,938
Carbon Monoxide	0	0	0	0
Nitrogen	0	736,951	0	749,851
Nitric Oxide	0	0	0	6.5
Oxygen	0	223,768	0	171,647
Sodium Hydroxide	0	0	0.017	0
Carbon Dioxide	0	0	0	57,750
Nitrogen Dioxide	0	0	0	1.2
Acetic Acid	4,100	0	0	0
Urea	25,075	0	0	0

SO ₂	0	0	0	0.003
SO ₃	0	0	0	0.013
Sodium Sulfate	2,196	0	2,196	0
Lysine	6,300	0	0	0
Trisodium Phosphate	6,242	0	6,242	0
Glucose	15,000	0	0	0

Table C.4.7-1. Cyclone Separator Dimensions (Lapple, 1951)

Diameter, D (m)	1.50
Height of Inlet, H (m)	0.75
Width of Inlet, W (m)	0.38
Length of Body, L _b (m)	3.00
Length of Cone, L _c (m)	3.00
Dust Outlet Diameter, D _d (m)	0.38
Diameter of Vapor Exit, D _e (m)	0.75
Vortex Finder, S (m)	0.94

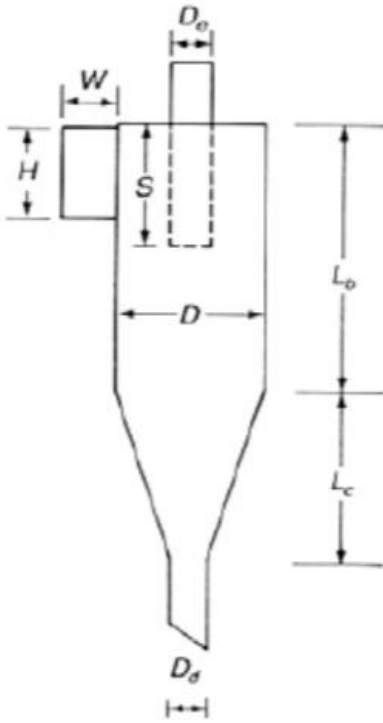


Figure C.4.7-1. Cyclone Diagram (Lapple, 1951)

10. References

- Afework, B., Hanania, J., Stenhouse, K., & Donev, J. (2018, September 3). *Cyclone separator—Energy Education*. Energy Education.
https://energyeducation.ca/encyclopedia/Cyclone_separator
- Aquanext. (2021). *The principle of desalination*. Aquanext. <http://www.aquanext-inc.com/en/product/desalination02.html>
- Average Weather in Dakar, Senegal, Year Round—Weather Spark*. (n.d.). Retrieved April 19, 2021, from <https://weatherspark.com/y/31520/Average-Weather-in-Dakar-Senegal-Year-Round>
- Boegger. (n.d.). *Feed Channel Spacers for Spiral-Wound Membranes in Reverse Osmosis*. Plastics Screen Mesh. Retrieved March 22, 2021, from <https://www.plasticscreenmesh.com/product/feed-spacer.html>
- Bosch, S., Struys, E. A., van Gaal, N., Bakkali, A., Jansen, E. W., Diederer, K., Benninga, M. A., Mulder, C. J., de Boer, N. K. H., & de Meij, T. G. J. (2018). Fecal Amino Acid Analysis Can Discriminate De Novo Treatment-Naïve Pediatric Inflammatory Bowel Disease From Controls. *Journal of Pediatric Gastroenterology and Nutrition*, 66(5), 773–778. <https://doi.org/10.1097/MPG.0000000000001812>
- Burga, D. (n.d.). *The Janicki Omni Processor: A Revolutionary Waste Management Innovation / The Cornell Healthcare Review*. Retrieved October 6, 2020, from <https://blogs.cornell.edu/healthreview/2020/03/08/the-janicki-omni-processor-a-revolutionary-waste-management-innovation/>
- Carlson, E. C. (1996). Don't Gamble With Physical Properties For Simulations. *CHEMICAL ENGINEERING PROGRESS*, 12.

- Carr, R. (2001). Water Quality: Guidelines, Standards, and Health. In L. Fewtrell & J. Bartram (Eds.), *Excreta-related infections and the role of sanitation in the control of transmission* (pp. 89–113). IWA Publishing.
https://www.who.int/water_sanitation_health/dwq/iwachap5.pdf
- Chowdhry, A. (2015, January 10). *Watch Bill Gates Sip Water Made From Sewer Sludge [Updated]*. Forbes. <https://www.forbes.com/sites/amitchowdhry/2015/01/10/janicki-omniprocessor/>
- Dresser-Rand steam turbines—A Siemens business*. (n.d.). [Newton_ps-detail]. Siemens-Energy.Com Global Website. Retrieved March 22, 2021, from <https://www.siemens-energy.com/global/en/offerings/power-generation/steam-turbines/d-r-steam-turbines.html>
- Environmental Protection Authority. (2004). *Photochemical smog—What it means for us*.
https://www.epa.sa.gov.au/files/8238_info_photosmog.pdf
- Fawell, J. K. (2007). *PH in Drinking-water*. World Health Organization (WHO).
- Feher, J. (2017). Osmosis and Osmotic Pressure. In *Quantitative Human Physiology* (2nd ed., pp. 182–198). Academic Press. <https://www.sciencedirect.com/topics/agricultural-and-biological-sciences/osmotic-pressure>
- Filtration + Separation. (2021, April 7). *Beneficial uses of concentrate waste*. Filtration + Separation. <https://www.filtsep.com:443/desalination/features/beneficial-uses-of-concentrate-waste/>
- Garg, A. (2004). Get the Most From Your Fired Heater. *Chemical Engineering*, 1–6.
- Geise, G. (2008, July). *RO/NF Membrane Characteristics*. Desalination Membrane Technology ICOM 2008 Workshop.
- GHG Online. (n.d.). *Other Greenhouse gases—NO_x*. Retrieved April 19, 2021, from

- <http://www.ghgonline.org/othernox.htm>
- Ho, V. (n.d.). *Your poo is (mostly) alive. Here's what's in it.* The Conversation. Retrieved February 28, 2021, from <http://theconversation.com/your-poo-is-mostly-alive-heres-whats-in-it-102848>
- Høverstad, T., Fausa, O., Bjørneklett, A., & Bøhmer, T. (1984). Short-chain fatty acids in the normal human feces. *Scandinavian Journal of Gastroenterology*, 19(3), 375–381.
- Ishaq, M. S., Afsheen, Z., Khan, A., & Khan, A. (2018). Disinfection Methods. *Photocatalysts - Applications and Attributes*. <https://doi.org/10.5772/intechopen.80999>
- Janicki, P. (n.d.-a). *The Omni Processor*. Retrieved November 6, 2020, from <https://swedishwaterhouse.se/wp-content/uploads/Peter-Janicki.pdf>
- Janicki, P. (n.d.-b). *The Omniprocessor*. Janicki Bioenergy. Retrieved February 28, 2021, from <https://swedishwaterhouse.se/wp-content/uploads/Peter-Janicki.pdf>
- Korsen21. (n.d.). *Energy use for membrane seawater desalination – current status and trends*.
- Lapple, C. E. (1951). Processes use many collector types. *Chemical Engineering*, 58(5), 144–151.
- Linerworld. (2009, March 12). *What Is Backwashing And What Is Its Purpose?* Linerworld. <https://blog.linerworld.com/2009/03/12/what-is-backwashing-and-what-is-its-purpose/>
- Nitto Group Company. (2021). *Hydranautics*. <https://www.imsdesign.com/Selection>
- Oregon Department of Human Services. (2000). *Technical Bulletin—Health Effects Information Ammonia*. Office of Environmental Public Health. <https://www.oregon.gov/oha/PH/HealthyEnvironments/DrinkingWater/Monitoring/Documents/health/ammonia.pdf>
- Peters, M. S., Timmerhaus, K. D., & West, R. E. (2003). *Plant Design and Economics for*

- Chemical Engineers* (5th ed.). McGraw-Hill Higher Education.
- Phys.org. (2015, September 23). *NO_x gases in diesel car fumes: Why are they so dangerous?*
<https://phys.org/news/2015-09-nox-gases-diesel-car-fumes.html>
- Poon, L. (2015, January 10). *Bill Gates Raises A Glass To (And Of) Water Made From Poop*.
 NPR.Org. <https://www.npr.org/sections/goatsandsoda/2015/01/10/376182321/bill-gates-raises-a-glass-to-and-of-water-made-from-poop>
- Project Overview / Sedron Technologies*. (n.d.). Retrieved November 4, 2020, from
<https://www.sedron.com/dakar-pilot/project-overview/>
- Puretec Industrial Water. (2021). *What is Reverse Osmosis?* Puretec Industrial Water.
<https://puretecwater.com/reverse-osmosis/what-is-reverse-osmosis>
- RO Chemicals. (2018). *Net Driving Pressure—Reverse Osmosis Systems*. Reverse Osmosis
 Chemicals. <http://reverseosmosischemicals.com/reverse-osmosis-guides/reverse-osmosis-glossary-terms/net-driving-pressure-reverse-osmosis-systems>
- Rose, C., Parker, A., Jefferson, B., & Cartmell, E. (2015). The Characterization of Feces and
 Urine: A Review of the Literature to Inform Advanced Treatment Technology. *Critical
 Reviews in Environmental Science and Technology*, 45(17), 1827–1879.
<https://doi.org/10.1080/10643389.2014.1000761>
- Salary Explorer. (2021). *Average Salary in Senegal 2021—The Complete Guide*.
<http://www.salaryexplorer.com/salary-survey.php?loc=192&loctype=1>
- Sanders, J.-G. (2018, November 6). *Omni Processor heading to commercial market*. GoSkagit.
https://www.goskagit.com/news/local_news/omni-processor-heading-to-commercial-market/article_a4dea2ca-4fee-55b5-b2d0-60a14331b7e0.html
- Selinidis, Y. (2019, January 7). *Introduction to Fired Heaters*. Scelerin Heaters.

<https://www.sclerlin.com/sclerlin-updates/2018/12/26/fired-heaters-101-a>

Senegal energy prices / *GlobalPetrolPrices.com*. (2020, January 3). GlobalPetrolPrices.Com.

<https://www.globalpetrolprices.com/Senegal/>

Simulation of Steam Engine with Aspen Plus V8.0. (2012, October 26).

<https://lms.nchu.edu.tw/sysdata/doc/9/9f7ce6465eb4c6e4/pdf.pdf>

Toray Industries, Inc. (2021). *Reverse Osmosis Basics*. Toray Water.

https://www.toraywater.com/knowledge/kno_001_01.html

Trading Economics. (2021). *Senegal Corporate Tax Rate*.

<https://tradingeconomics.com/senegal/corporate-tax-rate>

Turton, R. (2018). *Analysis, Synthesis, and Design of Chemical Processes* (5th Edition). Pearson Publishing.

United States Environmental Protection Agency. (2015a, May 29). *Ground-level Ozone Basics* [Overviews and Factsheets]. United States Environmental Protection Agency.

<https://www.epa.gov/ground-level-ozone-pollution/ground-level-ozone-basics>

United States Environmental Protection Agency. (2015b, December 23). *Overview of Greenhouse Gases* [Overviews and Factsheets]. United States Environmental Protection Agency. <https://www.epa.gov/ghgemissions/overview-greenhouse-gases>

United States Environmental Protection Agency. (2016, June 2). *Sulfur Dioxide Basics* [Overviews and Factsheets]. United States Environmental Protection Agency.

<https://www.epa.gov/so2-pollution/sulfur-dioxide-basics>

United States Environmental Protection Agency Office of Water. (2015, September 3). *Drinking Water Regulations and Contaminants* [Collections and Lists]. United States Environmental Protection Agency (US EPA). <https://www.epa.gov/sdwa/drinking-water->

regulations-and-contaminants

United States Environmental Protection Agency Office of Water. (2018). *2018 Edition of the Drinking Water Standards and Health Advisories Tables*.

United States National Park Service. (2018, September 11). *Sulfur Dioxide Effects on Health*.
<https://www.nps.gov/subjects/air/humanhealth-sulfur.htm>

Wanamaker, C. (2019, May). *How to Calculate Water Evaporation Loss in a Swimming Pool*.
Dengarden. <https://dengarden.com/swimming-pools/Determine-Evaporation-Rate-for-Swimming-Pool>

Water Vapor Pressure Chart. (n.d.). Retrieved April 19, 2021, from
http://www.msducanchem.com/Reference_Tables/water_vapor_pressure_chart.htm

WaterAnywhere. (2020). *CPA Series High Rejection—CPA Series Hydranautics Membranes*.
<https://wateranywhere.com/membranes/hydranautics-membranes/cpa-series-high-rejection/>

Where and how to buy land in Senegal. (2020, January 7). *JIWALL*.
<https://jiwall.com/en/acheter-une-maison-en/where-and-how-to-buy-land-in-senegal/>

Wikimedia Foundation. (2021). Osmotic pressure. In *Wikipedia*.
https://en.wikipedia.org/w/index.php?title=Osmotic_pressure&oldid=1010612681

Yacob, T. W., (Chip) Fisher, R., Linden, K. G., & Weimer, A. W. (2018). Pyrolysis of human feces: Gas yield analysis and kinetic modeling. *Waste Management*, 79, 214–222.
<https://doi.org/10.1016/j.wasman.2018.07.020>